AJNR

CT Features of Hyperostosing Meningioma En Plaque

Kwang S. Kim, Lee F. Rogers and David Goldblatt

AJNR Am J Neuroradiol 1987, 8 (5) 853-859
http://www.ajnr.org/content/8/5/853

CT Features of Hyperostosing Meningioma En Plaque

Kwang S. Kim[1]
Lee F. Rogers
David Goldblatt

Hyperostosis of the sphenoid ridge or convexity of the skull associated with meningioma en plaque (MEP) is often confused with other hyperostosing conditions, such as fibrous dysplasia or osteoma. The authors present nine cases, six of them proven, of hyperostosing MEP with specific attention to the CT features. All nine cases had one or more CT features that were characteristic or suggestive of MEP. These included periosteal pattern of hyperostosis, inward bulging of the vault lesion, surface irregularity of the hyperostotic bone, and intracranial changes.

The role of CT in evaluating MEP is compared with other neuroradiologic techniques. The results indicate that high-resolution CT is the neuroimaging method of choice in evaluating MEP.

Meningioma en plaque (MEP) provokes an adjacent bony hyperostosis that is often disproportionately greater than the relatively small underlying intracranial tumor [1, 2]. The bony hyperostosis produces clinical signs and symptoms by pressing against adjacent structures [1, 3]. Hyperostosis of the skull associated with MEP is often confused with other hyperostosing conditions such as fibrous dysplasia or osteoma. CT has established itself as a primary diagnostic technique for evaluating the brain and skull, yet literature describing CT features of hyperostosing MEP has been scant. We present nine cases, six of them proven, of hyperostosing MEP with specific attention to CT features. We also compare the role of CT with other neuroradiologic methods in the evaluation of hyperostosing MEP.

Materials and Methods

Nine cases of hyperostosing MEP were encountered during the period from May 1978 to June 1986. These included four cases (cases 1, 3, 8, 9) reported previously [4], which displayed a subdural layer of ossification as a characteristic feature of MEP. All nine cases had CT without and with infusion. Eight of these had CT with a high-resolution scanner, and one case (case 9) had an initial CT with an older-generation scanner and a follow-up CT 5 years later with a high-resolution scanner.

In all nine cases that had CT with a high-resolution scanner, the hyperostotic bone was evaluated with bone window settings that ranged from 400–1000 H in window level and 1800–3000 in window width.

All nine cases had plain skull films. Seven of these had a polytomogram of the hyperostotic bone and six had cerebral angiography. Two of the nine cases had MR (0.5 T, spin-echo, T1- and T2-weighted images).

Six (cases 1–6) of nine cases were surgically proven as hyperostosing meningioma en plaque. Tumor cells were present in the hyperostotic bone as well as in the subdural space in all six cases. The three unproven cases (cases 7–9) were diagnosed as hyperostotic meningioma en plaque on the basis of the age of the patient, clinical course, and characteristic radiographic findings, which included periosteal pattern of hyperostosis in case 7 and subdural ossification in cases 8 and 9.

This article appears in the September/October 1987 issue of *AJNR* and the November 1987 issue of *AJR*.

Received November 7, 1986; accepted after revision March 2, 1987.

[1] All authors: Department of Diagnostic Radiology, Northwestern University Medical School and Northwestern Memorial Hospital, Olson Pavillion, 710 North Fairbanks Court, Chicago, IL 60611. Address reprint requests to K. S. Kim.

***AJNR* 8:853–859, September/October 1987**
0195–6108/87/0805–0853

Results

Location of Hyperostosis. Hyperostosis was located in the sphenoid ridge in three cases, in the convexity in four cases, in the sphenoid ridge extending into the convexity in one case, and in the middle cranial fossa in one case. In three of five cases involving the convexity, hyperostosis was localized in the vicinity of the coronal suture. In the other two cases, hyperostosis covered an extensive area from the frontal region to the parietooccipital region.

Hyperostosis. Hyperostosis was sclerotic in all nine cases and was observed in four different patterns (Fig. 1). (1) Homogeneous pattern: Hyperostosis was of homogeneous density with the inner, middle, and outer tables ot distinguishable as separate structures. (2) Periosteal pattern: Hyperostosis was noted on the outer and/or inner surface of the skull. The adjacent table of the dense compact bone was distinguishable from the less dense hyperostotic bone. The adjacent table and the diploe were normal in thickness and density. (3) Three-layer pattern: Hyperostosis involved all three layers. The diploe remained less dense than the inner and outer layers, permitting all three layers to be distinguished. The overall thickness of the hyperostotic bone was rather moderate in degree in this pattern. (4) Diploic pattern: Hyperostosis involved the diploe, which was thickened and sclerotic. The outer and inner tables were distinguishable from the hyperostotic diploe, which was slightly less dense than the outer or inner table of the compact bone. The cortical definition of the outer and inner tables was normally preserved. Two or more patterns were present in the hyperostotic bone in four cases (cases 2, 5–7).

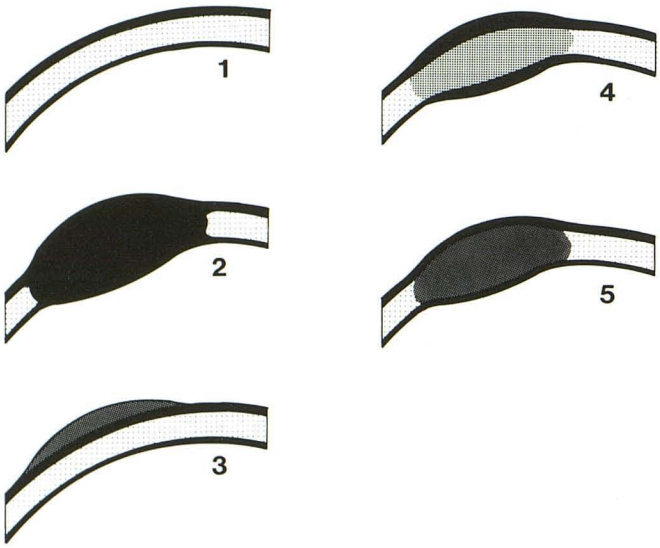

Fig. 1.—Graphic depiction of hyperostotic patterns. 1. Normal. 2. Homogeneous pattern: hyperostosis is of homogeneous density with the inner, middle, and outer tables not distinguishable. 3. Periosteal pattern: hyperostosis is noted on outer and/or inner surface of skull. The adjacent table of compact bone is distinguishable from the less dense hyperostotic bone. The adjacent tables and diploe are normal in thickness and density. 4. Three-layer pattern: hyperostosis involves all three layers. The diploe remains less dense than the inner and outer tables, permitting all three layers to be distinguished. 5. Diploic pattern: hyperostosis involves the diploe, which is slightly less dense than the outer or inner tables of compact bone. Cortical definition of outer and inner tables is normally preserved.

Inward Bulging of the Inner Aspect of the Hyperostotic Bone. In all five cases with the hyperostotic bone in the vault (cases 3–5, 7, 9), there was inward bulging of the inner aspect (see Figs. 3, 4, 6). In four of these, there was also outward bulging of the outer aspect, giving a biconvex appearance (see Figs. 3 and 4).

Surface Irregularity of the Hyperostotic Bone. Surface irregularity was present either on the inner and/or outer aspect of the hyperostotic bone in six cases (cases 2, 4–8) (Figs. 2A, 3, 4, 5D).

Intracranial Enhancing Mass. In three (cases 2, 4, 6) of nine cases the subdural meningiomatous plaque was directly visualized as a sheetlike enhancing mass along the plane of the meninges adjacent to the hyperostotic bone (Figs. 3B, 5A, 5D).

Subdural Ossification. In three cases (cases 1, 8, 9) a subdural layer of ossification along the hyperostotic bone with an intervening dural lucent line was noted. In case 9, the subdural ossification was not identified on the initial study performed with an older-generation scanner; however, it was subsequently shown on a follow-up study performed with a newer-generation scanner (Fig. 6A).

Mass Effect on the Brain. In five cases (cases 3–5, 7, 9) with a hyperostotic bone in the vault, there were varying degrees of mass effect on the brain from subtle flattening of the cortical sulci beneath the hyperostotic bone to a gross midline shift (Figs 3A and 3B).

Cerebral Edema. In one case (case 3), an area of vasogenic edema was present in the brain adjacent to the large hyperostotic bone in the convexity. The clinical and CT features of the cases are summarized in Table 1; cases 1–6 were surgically proven and cases 7–9 were unproven.

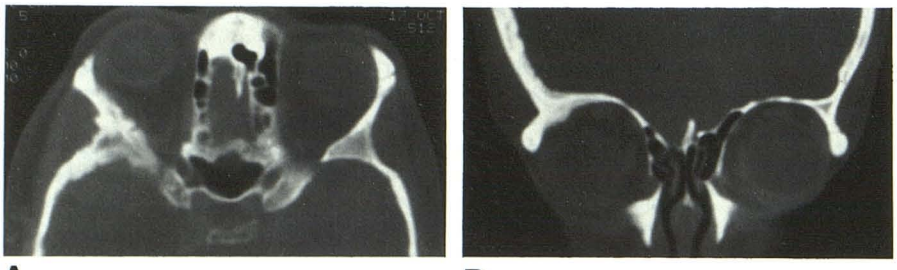

Fig. 2.—Case 2. CT scans at bone window settings in axial (*A*) and coronal (*B*) views show periosteal hyperostosis (periosteal pattern) along inner and orbital surfaces of greater sphenoidal wing. Adjacent inner and outer (orbital aspect) tables of compact bone are distinguishable from less dense hyperostotic bone. The diploe is not hyperostotic. There is surface irregularity of the hyperostotic bone. Three-layer pattern of hyperostosis is noted in skull superior to sphenoid wing in coronal view (*B*).

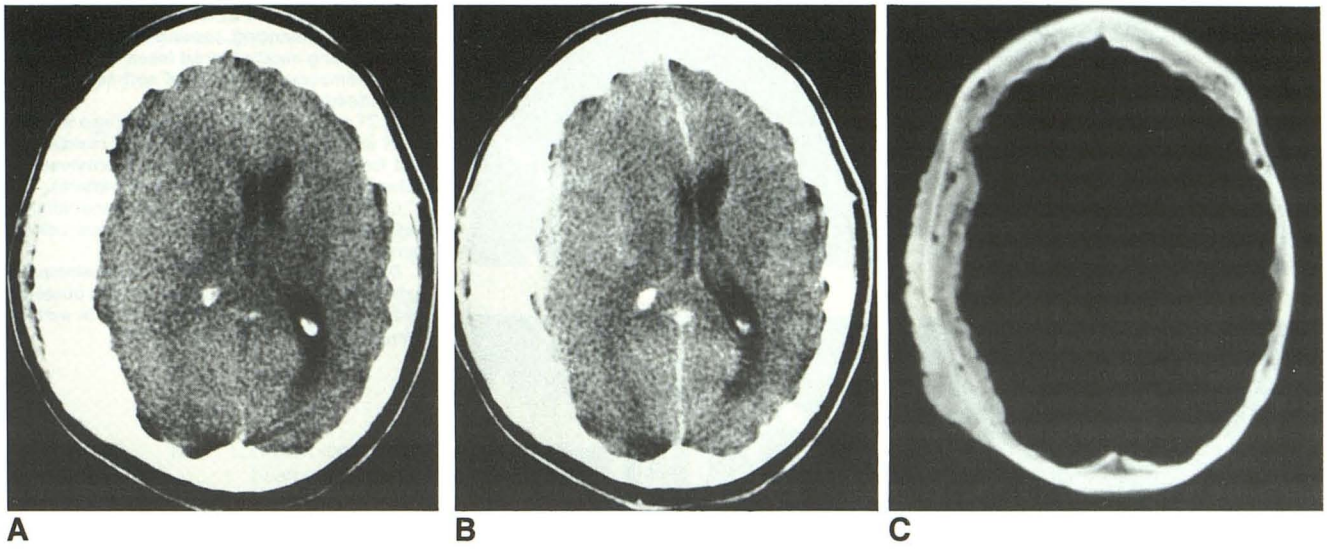

Fig. 3.—Case 4.

***A* and *B*, CT scans without (*A*) and with (*B*) infusion of contrast medium show extensive hyperostosis in frontoparietal region on right. There is enhancing subdural meningiomatous plaque along hyperostotic bone. Right lateral ventricle is compressed and midline structures are displaced to left.**

***C*, CT scan with bone window settings at same level shows periosteal reactive bone (periosteal pattern) on inner and outer aspect of skull. Adjacent outer table of compact bone is distinguishable from less dense hyperostotic bone. Adjacent inner table is in some areas distinguishable from hyperostotic bone while in others the inner table blends with the hyperostotic bone. The diploe is intact. Note presence of intradiploic veins shown as dotlike lucencies. There is surface irregularity of the hyperostotic bone.**

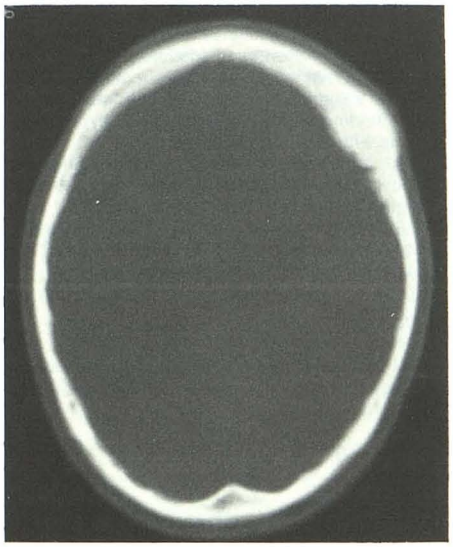

Fig. 4.—Case 5. CT scan with bone window settings shows hyperostosis in left frontoparietal region in vicinity of coronal suture. Hyperostosis is of homogeneous density with inner, middle, and external tables not distinguishable as separate structures (homogeneous pattern). The hyperostotic bone shows a biconvex appearance. There is surface irregularity on inner aspect of hyperostotic bone.

Other Neuroradiologic Investigations

Plain Skull Films. The plain skull films were available in all cases. In two (cases 1, 6) of nine cases hyperostosis was not recognized, even in retrospect. In the other seven cases, hyperostosis was identified but its specific pattern could not be determined. In one case (case 4), pressure atrophy of the sella turcica in addition to hyperostosis in the convexity was noted. In another case (case 6) with MEP in the middle cranial fossa, the skull films showed the extracranial portion of the soft-tissue mass in the infratemporal region bowing the wall of the ipsilateral maxillary sinus.

Polytomograms. Polytomograms were obtained in seven of nine cases, and hyperostosis was recognized in all seven. Details of hyperostotic pattern and recognition of the individual layer of the hyperostotic bone were limited when compared with high-resolution CT. However, detection of subdural ossification was comparable to that of high-resolution CT and superior to the older-generation CT.

Cerebral Angiograms. In six of nine cases, cerebral angiograms were available for review. No tumor stain or encasement of arteries was noted in any case. Nonspecific displacement of the intracranial vessels was noted in three. In one case (case 3), the middle meningeal artery on the side of the lesion was hypertrophic.

MR. Two cases (cases 5, 9) had MR, which did not show the intracranial meningomatous plaque in either case. CT did not detect the intracranial portion of the tumor as an enhancing mass in these cases. Demonstration of mass effect on the brain was comparable to that of CT. In case 5, the homogeneous hyperostotic bone in the convexity seen on CT was shown as a homogeneous low-signal area. However, the fine surface irregularity on the inner aspect of the hyperostotic bone seen on CT was not demonstrated on MR. In case 9, the diploic pattern of hyperostosis in the vault seen on CT was well demonstrated on MR (Fig. 6B). The thickened diploe

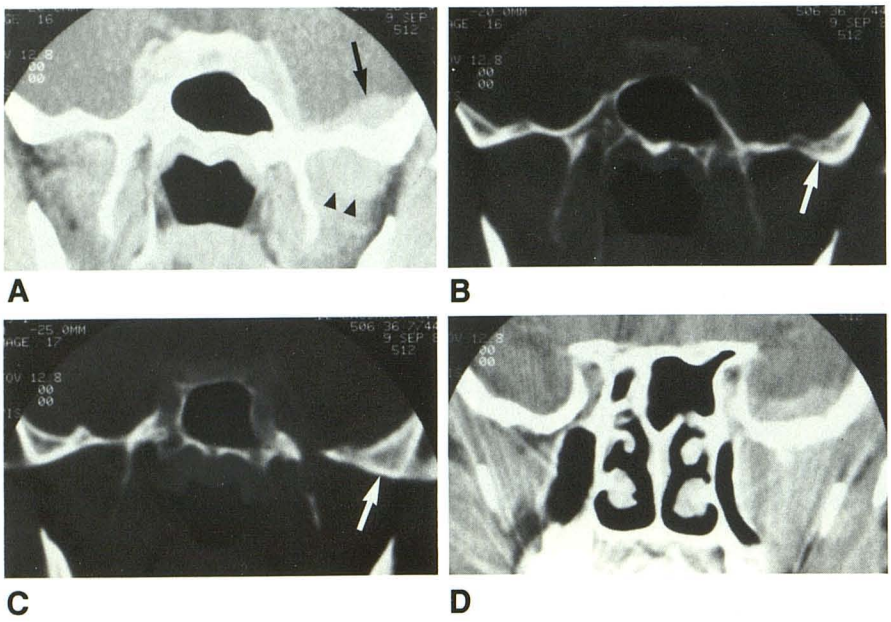

Fig. 5.—Case 6. ***A*****, CT scan with infusion shows an enhancing meningiomatous plaque (*arrow*) along middle cranial fossa on left. There is infratemporal extension of soft-tissue tumor (*arrowheads*).**

B**, CT scan with bone window settings at same level shows subtle hyperostosis of middle cranial fossa on left (*arrow*). The hyperostosis involves all three layers (three-layer pattern).**

C**, Section posterior to *A* with bone window settings shows diploic pattern of hyperostosis (*arrow*).**

D**, Section anterior to *A* shows infratemporal extension of soft-tissue tumor, bowing posterior lateral wall of maxillary sinus. There is surface irregularity of the hyperostotic bone.**

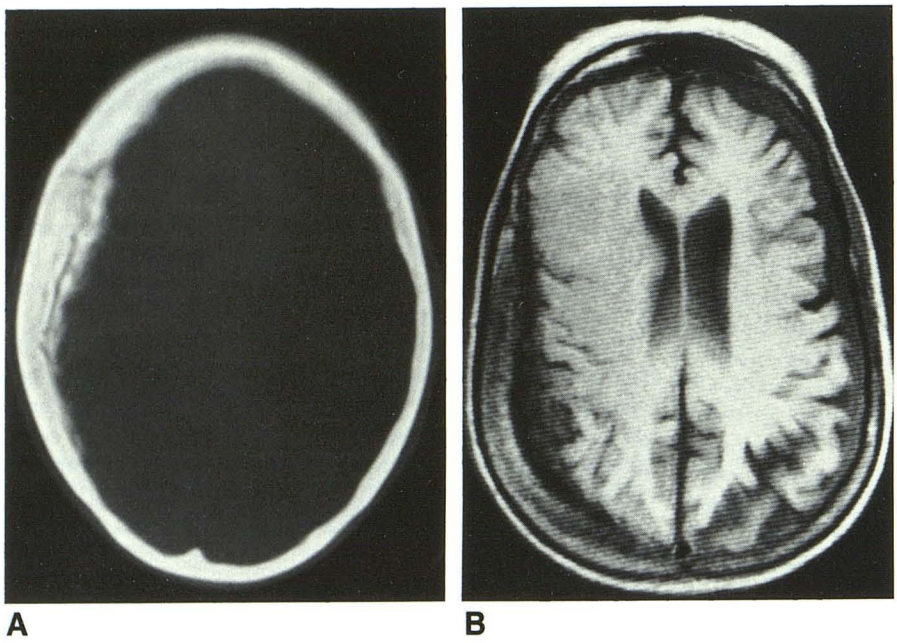

Fig. 6.—Case 9.

A**, CT scan with bone window settings shows extensive hyperostosis in frontoparietal region on right. Hyperostosis involves the diploe. The inner and outer tables of compact bone are distinguishable from slightly less dense diploe and are normally preserved (diploic pattern). There is inward bulging of inner aspect of hyperostotic bone. In addition, there is a subdural layer of ossification along inner aspect of hyperostotic bone with dural lucent interface.**

B**, MR (T1-weighted) at corresponding level shows thickened diploe as an area of relatively high signal intensity between outer and inner tables of low signal intensity. Subdural layer of ossification seen on CT is poorly defined and intervening dural lucent line is not shown.**

was shown as an area of relatively high signal intensity whereas the outer and inner tables of the compact bone appeared as zones of low signal intensity. However, the subdural layer of ossification along the inner aspect of the hyperostotic bone seen on CT was poorly defined and the intervening dural lucent line was not demonstrated on MR.

Discussion

Meningioma en plaque (MEP) is a tumor of limited thickness that grows along the planes of the meninges and, in some cases, occupies a considerable area [5]. MEP commonly occurs along the sphenoid ridge or the convexity [1, 5]. MEPs are more likely to provoke adjacent bony hyperostosis from tumor invasion than are the larger globoid tumors [1, 2]. The bony hyperostosis associated with MEP is characterized by indolent growth [3] and is always sclerotic [3, 6, 7]. Previous radiographic descriptions of hyperostosis associated with MEP have been sketchy and based on plain film or tomographic findings. High-resolution CT with bone window settings offers exquisite bony detail.

Hyperostosis associated with MEP in the sphenoid ridge is

TABLE 1: Clinical and CT Features of Hyperostosing Meningioma En Plaque

Case No.	Age	Gender	Symptoms	Site	Hyperostotic Bone			Intracranial Changes			
					Type of Hyperostosis	Surface Irregularity	Inward Bulging (Convexity Lesion)	Enhancing Mass	Subdural Ossification	Pressure Effect	Cerebral Edema
1	36	F	Blurred vision for 2 months	Sphenoid ridge	Three-layer	−		−	+	−	−
2	30	M	Exophthalmos, decreased visual acuity for 10 months	Sphenoid ridge	Homogeneous periosteal three-layer diploic	+		+	−	−	−
3	47	M	Lump on forehead for several years	Frontoparietal region in vicinity of coronal suture	Homogeneous	−	+	−	−	+	+
4	37	F	Headache for 2 months	Frontoparieto-temporal regions	Periosteal	+	+	+	−	+	−
5	40	F	Lump on forehead for 3 years	Frontoparietal region in vicinity of coronal suture	Homogeneous diploic	+	+	−	−	+	−
6	53	M	Facial swelling for 6 months	Middle cranial fossa	Three-layer diploic	+		+	−	−	−
7	46	F	Exophthalmos for 5 years	Sphenoid ridge	Periosteal	−		−	−	−	−
				Frontoparietal region in vicinity of coronal suture	Homogeneous three-layer	+	+	−	−	+	−
8	60	F	Exopthalmos for 3 years	Sphenoid ridge	Homogeneous	+		−	+	−	−
9	90	F	No symptoms	Frontoparieto-occipital regions	Diploic	−	+	−	+	+	−

Note.—Cases 1–6 were surgically proven and cases 7–9 were not proven.

commonly confused with fibrous dysplasia. Two (cases 7, 8) of our four cases with MEP in the sphenoid ridge had been diagnosed elsewhere as fibrous dysplasia prior to referral to our institution. Two (cases 3, 5) of five cases with convexity MEP had been confused with either osteoma or fibrous dysplasia.

The purpose of our classification of hyperostotic pattern was to find differential features from other hyperostosing conditions, such as fibrous dysplasia or osteoma. There was no relationship between the hyperostotic pattern and histologic type of MEP. Our own experience and review of the literature [6, 8–10] suggest that the hyperostotic patterns associated with MEP are similar to those of globoid meningiomas.

The periosteal hyperostotic pattern (Figs. 1–3) was observed in three cases (cases 2, 4, 7), two in the sphenoid ridge and the other in the vault. The inner and outer tables of the compact bone were distinguishable from the less dense hyperostotic bone. The normal cortical definition of the outer and/or inner tables was preserved. The new bone growth probably resulted from periosteal stimulation by tumor invasion. When this type of hyperostotic pattern is present, differentiation from fibrous dysplasia is virtually assured. Fibrous dysplasia should not give rise to periosteal new bone formation.

In the three-layer pattern (Figs. 1–4, 5B), the involvement of the inner table is a feature that may differentiate MEP from fibrous dysplasia. However, this feature is valid only when the hyperostosis is located in the convexity and the degree of hyperostosis is substantial. Only one of four cases with the

three-layer pattern had a convexity lesion, and in this case hyperostosis of the inner table was mild in degree.

Other patterns of hyperostosis do not serve to differentiate MEP from fibrous dysplasia on the basis of the type of pattern alone. However, inward bulging of the inner aspect of the hyperostotic bone is a feature that may serve to differentiate these conditions when the vault is the site of the lesion (Figs. 3, 4, 6). This feature was observed in five cases (cases 3–5, 7, 9). In fibrous dysplasia involving the convexity, the inner table is usually spared and a localized inward bulging of the inner table is rare [11].

An interesting feature associated with the hyperostosing MEP in the convexity is that the tumor is often localized in the vicinity of the coronal suture (Fig. 4). This has been observed by other investigators [12] and was present in three (cases 3, 5, 7) of five cases with hyperostosis in the vault in our series. In the other two cases (cases 4, 9), hyperostosis involved a wide area of the cranial vault, including the coronal suture (Figs. 3 and 6).

Another useful feature in the differentiation from fibrous dysplasia is the surface irregularity in the hyperostotic bone associated with MEP (Figs. 2A, 3, 4, 5D). In fibrous dysplasia, the surface of hyperostosis tends to be smooth [6, 13]. Surface irregularity was observed in six of nine cases (cases 2, 4–8). This feature allowed two additional cases to be differentiated from fibrous dysplasia.

There is superficial similarity between homogeneous hyperostosing MEP and osteoma in the cranial vault. However, differentiation between these two conditions should not be difficult. Osteoma usually arises from the outer table of the skull and rarely from the inner table [14]. Osteoma does not, as a rule, extend into the diploe [6, 15]. A biconvex appearance with inward and outward bulging has not been reported in osteoma. Another differential point is that osteomas do not extend across suture lines, whereas hyperostosis from meningiomas may cross suture lines [9]. Thus eight of our nine cases of MEP could be differentiated from fibrous dysplasia or osteoma on the basis of CT appearance of hyperostosis alone.

CT also provides excellent demonstration of the intracranial changes associated with MEP. Demonstration of an enhancing intradural plaque (Figs. 3B, 5A, 5D) or a subdural layer of ossification [4] (Fig. 6A) is characteristic of MEP. Another differential feature was pressure effect on the brain (Figs. 3A and 3B). This was seen in five cases, all with the lesion in the convexity. The pressure effect on the brain was due to inward bulging of the hyperostotic bone. In fibrous dysplasia involving the convexity, the curvature of the inner table is normally preserved and the presence of pressure effect on the brain is unusual [11].

The presence of cerebral edema is another valid differential feature from fibrous dysplasia or osteoma. However, cerebral edema was seen in only one (case 3) (11%) of nine cases with MEP. This is compared with an incidence of 46% [16] to 73% [17] with the globoid meningioma.

Utilizing the above-described features of bony hyperostosis and intracranial changes, high-resolution CT facilitated the diagnosis of MEP in all nine cases.

The value of high-resolution CT in evaluating MEP was compared with that of other neuroradiologic imaging techniques. The plain skull film was of limited value. In two of 10 cases, the plain skull films failed to show hyperostosis associated with MEP. Hyperostosis shown on the plain skull films was nonspecific. In one case (case 4), the plain skull films showed pressure atrophy of the sella turcica, which was not shown on CT; however, CT showed an extensive hyperostosing lesion with a considerable degree of mass effect on the brain (Figs. 3A and 3B). The value of the plain skull films perhaps lies in their demonstration of the hyperostotic bone as a baseline study.

Polytomography was inferior to high-resolution CT in evaluating hyperostotic changes. Polytomography was unable to demonstrate details of the individual layers of the skull or the relationship between the hyperostotic bone and the skull tables. No additional information was obtained by polytomography.

Cerebral angiography was disappointing. No tumor stain, encasement of the arteries by the tumor, or other diagnostic features were observed. In one case (case 3), enlargement of the middle meningeal artery was present. Enlargement of the middle meningeal artery is nonspecific for meningioma and it may be seen in fibrous dysplasia. In our opinion, cerebral angiography is not helpful in the diagnostic evaluation of MEP.

The value of MR in evaluating MEP is uncertain. It is known that MR is less sensitive than CT in detecting calcification or bony changes. MR's sensitivity in detecting the intracranial meningiomatous plaque is yet to be determined. MEP is a sheetlike tumor and MR has been known to be relatively insensitive in detecting small meningiomas. MR is probably more sensitive than CT in detecting cerebral edema associated with MEP. However, the presence of cerebral edema occurred in only one (11%) of nine cases in our series.

A hyperostosing MEP in the cranial vault is readily amenable to radical excision. This is more difficult in the sphenoid ridge. However, wide excision of the involved bone in the sphenoid ridge with successful results has recently been reported [18]. Therefore, preoperative anatomic definition of the involved bone is important and best obtained by high-resolution CT. At surgery, the outer surface of the dura beneath the hyperostosing bone may appear smooth and deceptively normal, as encountered in one (case 5) of our cases and by Toledo et al. [12]. Here, the preoperative diagnosis or a high degree of suspicion of hyperostosing MEP is essential so that at surgery the dura is incised and the subdural space is explored.

In summary, high-resolution CT is the neuroimaging method of choice in evaluating MEP. All nine cases had one or more CT features that were characteristic or suggestive of MEP. Polytomography does not provide any additional information. Cerebral angiography is not useful in establishing the diagnosis of MEP. The value of MR in detecting the intracranial portion of the tumor is yet to be proved.

REFERENCES

1. Cushing H. The cranial hyperostoses produced by meningeal endotheliomas. *Arch Neurol Psychiatry* **1922**;8:139–154

2. Russell DS, Rubinstein LJ. Pathology of tumors of the nervous system. Baltimore: Williams & Wilkins, **1979**
3. Castellano F, Guidetti B, Olivecrona H. Pterional meningioma "en plaque." *J Neurosurg* **1952**;9:188–196
4. Kim KS, Rogers LF, Lee C. The dural lucent line: characteristic sign of hyperostosing meningioma en plaque. *AJNR* **1983**;4:1101–1105
5. Boldrey E. The meningiomas. In: Minkler J, ed. *Pathology of nervous system*, vol 2. New York: McGraw-Hill, **1971**:2125–2144
6. Burrows EH, Leeds NE. *Neuroradiology*, vol 1. New York: Churchill Livingstone, **1981**:1–74
7. Cushing H, Eisenhardt L. *Meningiomas: their classification, regional behavior, their life history and surgical end result*. Springfield, IL: Thomas, **1938**
8. Ethier R. Skull vault: thickness and texture. In: Newton TH, Potts DG, eds. *Radiology skull and brain*, vol 1. St. Louis: Mosby, **1971**:154–215
9. Pendergrass EP, Perryman CP. Roentgenologic aspects of meningiomas. *Br J Radiol* **1952**;15:225–234
10. Traub SP. *Roentgenology of intracranial meningioma*. Springfield, IL: Thomas, **1961**
11. Leeds N, Seaman WB. Fibrous dysplasia of the skull and its differential diagnosis: a clinical and roentgenographic study of 46 cases. *Radiology* **1962**;78:570–582
12. Toledo E, Dujovny M, Isreali JB. Cranial vault hyperostosis overlying meningioma "en plaque." *Isr J Med Sci* **1973**;9:62–66
13. Banna M, Appleby A. Some observations on the angiography of supratentorial meningiomas. *Clin Radiol* **1969**;20:375–386
14. Wilner D. *Radiology of bone tumors and allied disorders*, vol 1. Philadelphia: Saunders, **1982**:82
15. Taveras JM, Wood EH. *Diagnostic neuroradiology*, vol 1, 2nd ed. Baltimore: Williams & Wilkins, **1976**:120
16. Stevens JM, Ruiz JS, Kendell BE. Observations on peritumoral edema in meningioma, part 1. *Neuroradiology* **1983**;25:71–80
17. Bradac GB, Ferszt R, Bender A, Schorner W. Peritumoral edema in meningiomas: a radiological and histological study. *Neuroradiology* **1986**;28:304–312
18. Pompili A, Deroma PJ, Visot A, Guiot G. Hyperostosing meningiomas of the sphenoid ridge—clinical features, surgical therapy, and long-term observations: review of 49 cases. *Surg Neurol* **1981**;17:411–416